The Electronic Structure of Magnesium Dialuminium Tetraoxide (Spinel) using *X*-Ray Emission and *X*-Ray Photoelectron Spectroscopies

By **Derek E. Haycock, Christopher J. Nicholls, David S. Urch,* and M. J. Webber,** Chemistry Department, Queen Mary College, Mile End Road, London E1 4NS
Gerhardt Wiech, Department of Physics, University of Munich, 8 Munich 22, 1 Geschwister-Scholl-Platz, West Germany

The Mg-$K_{\beta_{1,3}}$, O-$K_{\alpha_{1,2}}$, Al-$K_{\beta_{1,3}}$ and Al-$L_{2,3}$ *X*-ray emission spectra and also the *X*-ray photoelectron spectrum of spinel, $MgAl_2O_4$, are reported. A model for the bonding is derived using simple molecular-orbital theory, which is adequate for a qualitative rationalisation of the observed spectra. The shape of particular *X*-ray emission peaks is shown to be strongly dependent on the bonding commitments and co-ordination of the emitting atoms.

By means of *X*-ray emission spectroscopy [1,2] it is possible to investigate the bonding role of particular atomic orbitals from specified atoms. The Laporte selection rule ($\Delta l = \pm 1$) for the dipole component of electromagnetic radiation ensures that a vacancy in an *s* orbital shall be filled only by electronic transitions from *p* orbitals, a vacancy in a *p* orbital by transitions from *s* and *d* orbitals, *etc.* Furthermore, simple calculations suffice to demonstrate [3] that 'cross-over' transitions from ligand atoms are unimportant, *i.e.* the intensity of *X*-radiation that derives from an electronic transition from one atom to a vacancy on another is negligible. These preliminary considerations show that *X*-ray emission is essentially an atomic phenomenon, which can, however, be severely perturbed by molecular bond formation. Obviously those *X*-rays which result from electronic transitions from valence-band orbitals to inner vacancies will be the most affected. An atom A may make a variety of molecular orbitals (m.o.s) of different energies (E_1, E_2, . . . E_n) with say atom B. If valence-shell *p* orbitals of A contribute to these orbitals with coefficients (using the LCAO approximation) a_1, a_2, . . . a_n, then the structure of the A *K*-emission band that arises from the (valence band→A 1*s*) transition will be *n* peaks corresponding to *X*-rays with energies $E(A, 1s) - E_1$, $E(A,1s) - E_2$, . . . $E(A, 1s) - E_n$ and with relative intensities $(a_1)^2$, $(a_2)^2$, . . . $(a_n)^2$. If *p* character from B were found in the same m.o.s with coefficients b_1, b_2, • • • b_n then the structure of the corresponding *K*-emission peak for B would be a series of peaks of energies $E(B, 1s) - E_1$, $E(B, 1s) - E_2$, . . . $E(B, 1s) - E_n$, with relative intensities $(b_1)^2$, $(b_2)^2$, . . . $(b_n)^2$.

A study of the structure of individual *X*-ray peaks thus reveals the bonding commitments of particular atomic orbitals, but a much more complete dissection of the chemical bond can be obtained by assembling complimentary *X*-ray emission spectra of different types and from different atoms on a common energy scale.[4] For this to be possible, inner-orbital ionisation energies, *e.g.* $E(A, 1s)$, and $E(B, 1s)$, must be measured directly by means of *X*-ray photoelectron spectroscopy.[5,6] It must be emphasised, however, that data from both *X*-ray emission and *X*-ray photoelectron spectroscopies are obtained which relate to unipositive ions rather than to neutral molecules or structures. The same ions are produced by both techniques which is why the results can be directly correlated. The relation between these ions and the neutral species is extremely simple *if* Koopman's theorem [7,8] is obeyed, for in this case the experimental ionisation energy may be directly equated with the calculated SCF energy in the neutral molecule. Should this convenient axiom not hold, however, then the ion–neutral molecule correlation becomes uncertain. It will be assumed for the purposes of this paper that Koopman's theorem does hold, but no quantitative calculations are attempted.

In this paper the complimentary techniques of *X*-ray emission and *X*-ray photoelectron spectroscopy are used to build up a picture of the electronic structure of spinel, $MgAl_2O_4$. These studies follow naturally from the initial work on magnesium oxide.[9] The spinel structure [10] is more complex, the magnesium being tetrahedrally and aluminium octahedrally co-ordinated by oxygen, whilst each oxygen atom is bound to three aluminium and to one magnesium atom. Theoretical calculations using the SCF K_α method on isolated $[MgO_4]^{6-}$ (T_d) [11] and $[AlO_6]^{9-}$ (O_h) [12] units have been described by Tossell but very little experimental *X*-ray work has been reported previously on spinel. Freund and Hamich [13] and also Dodd and Glenn [14] have discussed the bonding of magnesium in spinel but each pair of workers based their arguments on Mg-$K_{\beta_{1,3}}$ spectra alone.

[1] A. H. Compton and S. K. Allinson, '*X*-Rays in Theory and Experiment,' Van Nostrand, New York, 1935.
[2] D. S. Urch, *Quart. Rev.*, 1971, **25**, 343.
[3] D. S. Urch, *J. Phys.* (*C*), 1970, **3**, 1275.
[4] R. E. LaVilla, *J. Chem. Phys.*, 1972, **57**, 899.
[5] K. Siegbahn, C. Nordling, R. Fahlman, R. Nordberg, K. Hamrin, J. Hedman, G. Johansson, T. Bergmark, S.-E. Karlsson, I. Lindgren, and B. Lindberg, 'ESCA-Atomic, Molecular and Solid State Structure Studies by Means of Electron Spectroscopy,' Almqvist and Wiksells, Uppsala, Sweden, 1967.
[6] A. D. Baker, C. R. Brundle, and M. Thompson, *Chem. Soc. Rev.*, 1972, **1**, 355.
[7] T. Koopmans, *Physica*, 1934, **1**, 104.
[8] W. G. Richards, *Internat. J. Mass Spectrom. Ion Phys.*, 1969, **2**, 419.
[9] C. J. Nicholls and D. S. Urch, *J.C.S. Dalton*, 1975, 2143.
[10] W. H. Bragg, *Phil. Mag.*, 1915, **30**, 305.
[11] J. A. Tossell, *J. Amer. Chem. Soc.*, 1975, **97**, 4840.
[12] J. A. Tossell, *J. Phys. and Chem. Solids*, 1975, **36**, 1273.
[13] F. Freund and M. Hamich, *Z. anorg. Chem.*, 1971, **385**, 209.
[14] C. G. Dodd and G. L. Glenn, *J. Appl. Phys.*, 1968, **39**, 5377.

Freund and Hamich suggested that π orbitals were more tightly bound than related σ orbitals, whilst Dodd and Glenn invoked a dipole-forbidden $3s$—$1s$ transition in order to explain the observed structure of the Mg-$K_{\beta_{1,3}}$ emission peak. Neither of these unreasonable suggestions is needed if a more detailed study of the bonding, based on more comprehensive experimental data, is made.

EXPERIMENTAL

Very small pink crystals of spinel (ref. no. B.M. 1911 705; location, India) were kindly supplied by the Mineralogical Department of the British Museum (Natural History). The crystals were carefully ground to a fine powder in an agate mortar. The powdered spinel was pressed into a thin copper mesh for the determination of the O-K_α and Mg-$K_{\beta_{1,3}}$ spectra. Al-$K_{\beta_{1,3}}$ was measured from a sample mounted on double-sided Sellotape which had previously been used for X-ray photoelectron spectroscopy. The conventional X-ray emission measurements were made on a Philips PW 1410 spectrometer using a chromium-anode X-ray tube (50 kV, 50 mA). All the spectra were obtained using a step-scanning technique in which data were collected at a fixed wavelength for a predetermined time. When this information had been printed out the wavelength was changed automatically and the counting procedure repeated. In each case the best resolution was achieved by choosing crystals which would reflect the X-rays of interest at high angles: O-K_α, rubidium acid phthalate ($2d$ = 2.612 nm), first order; Mg-$K_{\beta_{1,3}}$, ammonium dihydrogenphosphate ($2d$ = 1.064 nm), first order; and Al-$K_{\beta_{1,3}}$, ethylenediamine tartrate ($2d$ = 0.881 nm), first order.

Fine Soller-slit collimation was used (150 μm between blades giving a maximum angular divergence of just less than $\pm 0.1° \theta$). Under these conditions the overall resolving power of the instrument ($E/\Delta E$) was, very approximately, 400, giving peak widths [full width at half-height (f.w.h.h.)] of 1, 3, and 4 eV for O-K_α, Mg-$K_{\beta 1,3}$, and Al-$K_{\beta 1,3}$ respectively.* The X-rays were detected using a proportional counter (flow gas, 90% argon and 10% methane, at atmospheric pressure), fitted with a thin (1 μm) polyester window. Amplification and counting equipment was from the Harwell 2000 series. Results were plotted on an energy scale of 1 cm ≡ 1 eV. This enabled all the different X-ray spectra to be directly compared (Figure 1).

In order to measure the aluminium $L_{2,3}$ M spectrum at 160—280 Å (45—75 eV) a soft X-ray grating spectrometer was used. This instrument has been fully described by Wiech.[15] The finely ground sample was pressed on to a copper block where it was subjected to direct electron bombardment (3 kV, 1 mA). The characteristic X-rays from the sample were analysed by means of a diffraction grating (radius, 1.999 5 m; 600 lines mm^{-1}; blaze angle, 1° 31′), and detected in a Bendix channel multiplier. The whole instrument was operated at a vacuum of better than 10^{-6} Torr. The spectrum was collected using a step-scanning technique.

X-Ray photoelectron spectroscopy was performed on a Vacuum Generators ESCA III spectrometer, using an aluminium-anode X-ray tube operated at 10 kV and 10 mA.

* Throughout this paper: 1 eV ≈ 1.60 × 10^{-19} J; 1 Torr = (101 325/760) Pa.

[15] G. Wiech, *Z. Phys.*, 1966, **193**, 490.

The powdered sample was mounted on the probe using double-sided Sellotape. However, the valence-band spectrum obtained in this way [Figure 1(*i*)] was without any

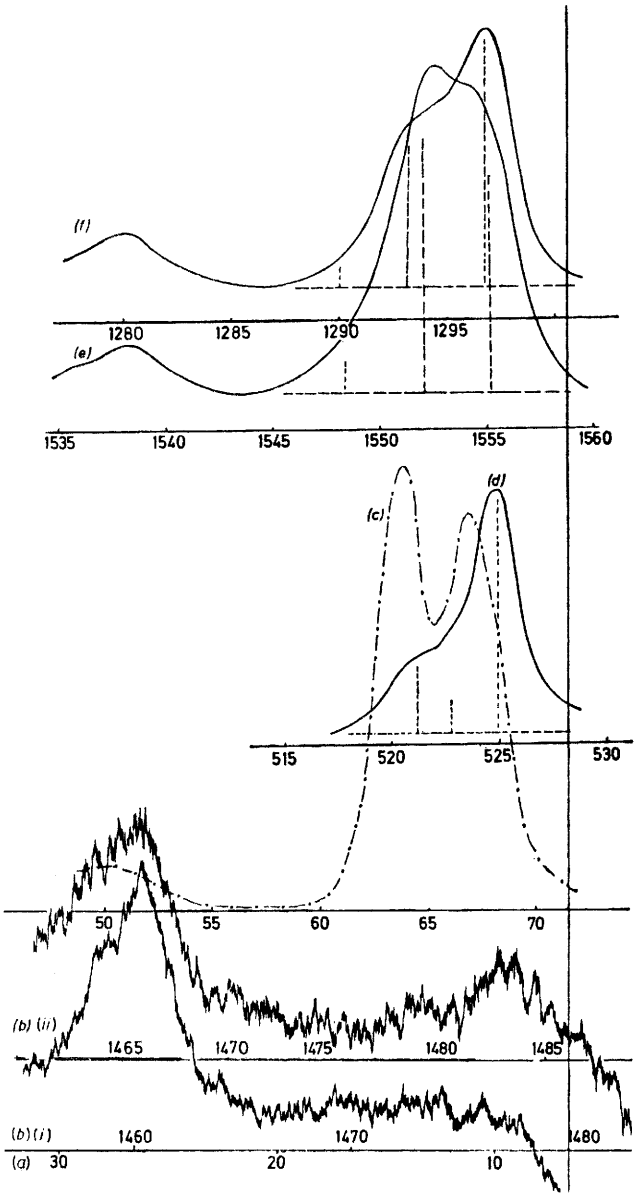

FIGURE 1 X-Ray photoelectron and X-ray emission spectra from spinel. The vertical scale for all the spectra is arbitrary. The various spectra are presented with their own energy scales (in eV) and correlated with one another using the photoelectron data of Table 1. (*a*) and (*b*), binding energies and electron kinetic energies for the valence-band photoelectron spectra: (*i*) from powdered spinel (India) mounted on Sellotape, (*ii*) from synthetic spinel crystal. (*c*)—(*f*), spectra of Al-$L_{2,3}$ M, O-$K_{\alpha 1,2}$ Al-$K_{\beta 1,3}$, and Mg-$K_{\beta 1,3}$. Spectra (*d*)—(*f*) show the assumed baseline and approximate positions and heights (broken lines) of the constituent peaks

discernible structure except for the oxygen 2s peak. A single crystal of synthetic spinel (kindly supplied by Professor Anderson, Imperial College, London), was therefore mounted directly at the end of the sample probe. The spectrum that resulted, after the crystal had been cleaned by argon-ion sputtering, is shown in Figure 1(*ii*). The Al 2p

and Mg 2*p* peaks were used to relate the photoelectron energy scales for the two spectra. For maximum peak intensities the spectrometer was operated with an analyser energy of 100 V which gives an effective Al-$K_{\alpha_{1,2}}$ linewidth (*i.e.* f.w.h.h.) of 1.8 eV. All the spectra were run under constant conditions (*i.e.* 30-V scans of 3 000-s duration with a ratemeter time constant of 10 s), in order that instrumental factors which might cause peak displacement should be constant. By far the most important cause of peak shift (apart from chemical effects) is, however, the charging of a non-conducting sample due to *X*-irradiation, especially in those experiments where the sample was insulated from the probe by Sellotape. It is interesting to note that the directly mounted spinel crystal gave photoelectrons for Al 2*p* and Mg 2*p* with a kinetic energy of 6.0 ± 0.1 eV greater than those from the Sellotape sample. This indicates, that although spinel is itself an insulator, the use of Sellotape as a mounting medium is the major factor in giving a highly charged sample. It is experimentally difficult to determine the exact charge carried by a specimen [16-18] although many techniques have been proposed. The carbon peak reported with the *X*-ray photoelectron spectroscopic data in Table 1 gives some indication of the sample charge, but no attempt was made to either dispel or to measure the charge in these experiments since the essential information required to align

TABLE 1

Atomic-orbital binding energies in spinel

Orbital	Binding energy (eV)	Full width at half-height (eV)	Notes
Al 2*p*	78.3 (72.4)	2.7	
Al 2*s*	123.0	3.0	
Al 1*s*			Al 1*s* = Al 2*p* + Al-K_α (spinel) = 78.3 + 1 487.1 = 1 565.4
Mg 2*p*	54.0 (47.8)	2.6	Mg-K_α = Mg 1*s* − Mg 2*p* = 1 307.6 − 54.0 = 1 253.6
Mg 2*s*	92.9 (87.0)	2.8	
Mg 1*s*	1 307.6	3.5	[Mg-K_α (spinel) (expt) = 1 253.8]
O 1*s*	534.8	3.0	
C 1*s*	288.4	3.0	

Figures in parentheses are for a crystal of synthetic spinel.

the *X*-ray emission spectra is a knowledge of the differences in the orbital ionisation energies of the different atoms in the sample. The ' zero level ' in Figure 1 has, therefore, no absolute significance: it is presumably the effective Fermi level of spinel whilst under irradiation in the spectrometer.

RESULTS AND DISCUSSION

X-Ray photoelectron data are summarised in Table 1 and the *X*-ray emission results together with the valence-band spectrum are presented graphically in Figure 1. In this Figure the individual spectra have been aligned using the photoelectron data from the Table. All the *X*-ray emission peaks show some degree of structure, reflecting in each case at least two distinct bands of molecular orbitals. The broken lines under some of the experimental curves in Figure 1 show the heights and locations of Gaussian peaks indicated by the use of a Du Pont 310 curve resolver and also by a simple curve-synthesis computer program; full details of the results of curve resolution are given in Table 2. The

TABLE 2

Curve resolution for O-K_α, Mg-K_β, and Al-K_β

Peak	Energy (eV)	Relative intensity	Full width at half-height (eV)
O-K_α	521.2	286	4.26
	522.7	143	2.30
	524.9	1 000	2.92
Mg-$K_{\beta_{1,3}}$	1 290.1	83	3.29
	1 293.3	572	3.80
	1 294.9	174	2.81
	1 296.9	1 000	3.64
Al-$K_{\beta_{1,3}}$	1 548.6	133	5.15
	1 552.3	1 264	4.92
	1 555.2	1 000	4.51

relative intensities of the component peaks revealed in this way are quite different for magnesium and aluminium, indicating different bonding commitments for the 3*p* orbitals of these two elements in spinel.

This is in qualitative agreement with the calculations of Tossell for magnesium in tetrahedral [11] and aluminium in octahedral [12] co-ordination sites. The two components of Al-$K_{\beta_{1,3}}$ at 1 552.3 and 1 555.2 eV may be identified with $5t_{1u}$ and $6t_{1u}$ in $[AlO_6]^{9-}$. The relative amounts of charge density found at the metal (M) and in the interatom (bond) region (II) for these two orbitals are, respectively, 2.0 and 1.0 (M) and 41 and 17 (II). Such a great variation in Al 3*p* character is not observed in the Al-$K_{\beta_{1,3}}$ spectrum, but the more tightly bound m.o. is associated with the more intense component of the peak. For magnesium the peaks at 1 293.3 and 1 296.9 eV are derived from transitions from the $4t_2$ and $5t_2$ molecular orbitals. In this case the calculations show relative intensities of 1.0 and 2.0 (M) but 38.0 and 21.4 (II) for the interatom region. Experimentally, the transitions from $5t_2$ are more intense than those from $4t_2$, in agreement with the calculated charge distribution in the region of the magnesium atom. The calculated energy differences between $5t_{1u}$ and $6t_{1u}$ appear to be of the right order (*ca.* 3 eV) for aluminium in spinel but for magnesium the $4t_2$—$5t_2$ energy separation (*ca.* 2 eV) is too small. This is probably because interactions between $[AlO_6]^{9-}$ and $[MgO_4]^{6-}$ *via* bridging oxygen atoms have not been considered. Any attempt to describe the electronic structure of spinel should, therefore, take account of interactions between the $[AlO_6]^{9-}$ and $[MgO_4]^{6-}$ units.

Electronic Structure.—A suitable model for a discussion of the bonding in periclase (magnesium oxide) was found to be Mg_4O_4, a cube with magnesium and oxygen atoms at alternate corners.[9] The structure of spinel can be thought of in a similar manner; Al_4O_4 cubes which are linked through shared oxygen atoms to MgO_4 tetrahedra.

[16] D. S. Urch and M. Webber, *J. Electron Spectroscopy*, 1974, **5**, 791.

[17] M. F. Ebel and H. Ebel, *J. Electron Spectroscopy*, 1974, **3**, 169.

[18] D. Betteridge, J. C. Carver, and D. M. Hercules, *J. Electron Spectroscopy*, 1973, **2**, 237.

For simplicity in visualising this description of the spinel structure MgO_4 can be regarded as a cube with oxygen atoms and vacancies at alternate corners and with a magnesium atom at the centre. Such an $MgAl_{16}O_{16}$ unit is shown diagramatically in Figure 2.

$MgAl_{16}O_{16}$ is, of course, not in any sense a ' unit cell ' or even a repeating unit from which the bulk crystal structure of spinel could be generated by replication, and also whilst the magnesium and a few of the oxygen atoms have their correct co-ordination none of the aluminium atoms in this model is six-co-ordinate. However, as will be discussed below, this model can be used to conveniently describe the electronic structure of spinel. Each aluminium atom can be regarded as sp hybridised with one hybrid orbital pointing towards the centre of the equilateral triangle generated by three neighbouring oxygens (an equilateral triangle that is

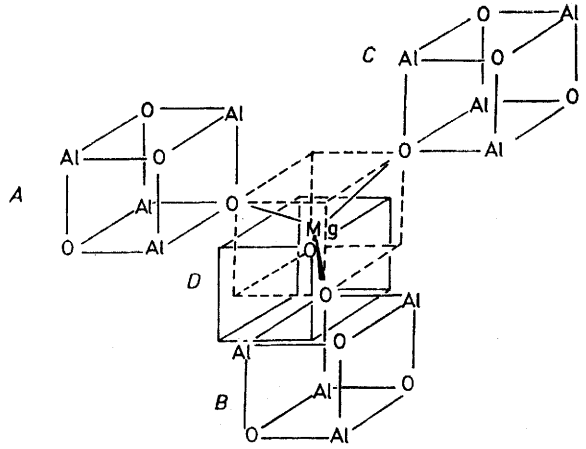

FIGURE 2 Representation of the crystal structure of spinel. Al and O atoms have been omitted from cube D for clarity

one of the faces of the octahedron of oxygen atoms that surrounds the aluminium). The other hybrid points towards the other three oxygens that are outside the $MgAl_{16}O_{16}$ unit. Since the sp hybrids are orthogonal so also will be their interactions with the two trios of oxygen atoms. Furthermore, the aluminium $3p$ orbitals tangential to the hybrids' axis can be shown to play little part in bonding. Thus interactions between one Al sp hybrid and three neighbouring oxygens can be regarded as representative of the bonding commitments of the aluminium atoms. A consideration of the bonding in the $MgAl_{16}O_{16}$ unit should therefore give a reasonable indication of the disposition of the various atomic orbitals amongst the m.o.s of spinel. As in the case of MgO, the bonding picture can be described in stages: first the bonding within each Al_4O_4 unit, and then the interactions of four such units with a magnesium atom.

Al_4O_4. It will be assumed that the oxygen $2s$ and $2p$ orbitals have such different ionisation energies (27 and 9 eV: see Figure 1) that their bonding interactions from other atoms can be considered separately and that the ionisation energies of Al $3s$ and $3p$ are sufficiently close that hybrid orbitals [*i.e.* $(0.5)^{-\frac{1}{2}}$(Al $3s \pm$ Al $3p$)] can be used without introducing gross errors into the subsequent calculations. Thus both the four aluminium sp hybrid orbitals orientated towards the centre of the cube and the four oxygen $2p$ orbitals that can also be directed to the centre will form sets of symmetry orbitals under their local tetrahedral symmetry that transform as the irreducible representations a_1 and t_2. Following the arguments presented for Mg_4O_4, it can be shown [9] that two sets of occupied m.o.s will be formed: a rather tightly bound a_1 orbital and a trio of degenerate orbitals (t_2) which are approximately non-bonding relative to the oxygen $2p$ atomic-orbital ionisation energy. In the limit of a wholly ionic bond, it can be shown (Appendix, ref. 9) that the (vanishingly small) Al $3(sp$ hybrid) coefficient in the a_1 orbital will be three times that in any one of the t_2 orbitals. In the limit, therefore, it follows that the Al $3(s,p$ hybrid) character will be found associated with the a_1 and t_2 orbitals in the ratio 3 : 1.

The overlap of orbitals tangential to the surface of the sphere which would contain all the eight atoms of Al_4O_4 will be much less than that between orbitals orientated towards the centre. The eight oxygen $2p$ orbitals of this type (e, t_1, and t_2) will, therefore, behave as lone pairs interacting only slightly with the corresponding family of aluminium $3p$ orbitals. The mutual repulsions between oxygen e, t_1, and t_2 orbitals will lead to slight differences in orbital-ionisation energies which will in turn be manifest in the shape and breadth of the main oxygen $K_{\alpha_{1,2}}$ emission peak.

MgO_4. Before the bonding between the magnesium atom and the surrounding tetrahedron of oxygen atoms can be considered it is necessary to investigate the nature of the oxygen p orbitals that project from each Al_4O_4 unit towards the magnesium. The four Al_4O_4 cubes in Figure 2 are identified as A—D and the $2p$ orbitals on the oxygen atom which acts as a bridge between each Al_4O_4 unit and the magnesium atom is given the number i; the other oxygen $2p$ orbitals which point towards the centre of a cube are then ii—iv. The four occupied bonding orbitals associated with an Al_4O_4 cube can thus be represented as in (1). (Explicit reference to the small aluminium $3s$ and $3p$ contributions to these orbitals has been omitted for simplicity in presentation.)

$$\begin{array}{ll} a_1 & 0.5(i + ii + iii + iv) \\ t_2 & \left\{\begin{array}{l} 0.5(i + ii - iii - iv) \\ 0.5(i - ii + iii - iv) \\ 0.5(i - ii - iii + iv) \end{array}\right. \end{array} \quad (1)$$

Since the three t_2 orbitals are degenerate it is possible to use any convenient set of linear combinations of the orbitals given above, *e.g.* (2).

$$t_2 \left\{\begin{array}{l} \alpha = (12)^{-0.5}[3(i) - ii - ii - iv] \\ \beta = (2)^{-0.5}(iii - iv) \\ \gamma = (6)^{-0.5}[2(ii) - iii - iv] \end{array}\right. \quad (2)$$

In selecting those orbitals in cubes A—D which will interact with the magnesium atom it is now only neces-

sary to consider the four a_1 orbitals [from equation (1)] and the four α [from equation (2)]. Each will give rise to symmetry orbitals belonging to irreducible representations a_1 and t_2, with respect to the tetrahedral symmetry

$$\begin{array}{ll} a_1 & 0.5(Aa_1 + Ba_1 + Ca_1 + Da_1) \\ t_2 & \left\{\begin{array}{l} 0.5(Aa_1 + Ba_1 - Ca_1 - Da_1) \\ 0.5(Aa_1 - Ba_1 + Ca_1 - Da_1) \\ 0.5(Aa_1 - Ba_1 - Ca_1 + Da_1) \end{array}\right. \end{array} \quad (3)$$

about the magnesium atom, of the type (3). An exactly similar set of orbitals can be generated from Al_4O_4 α orbitals by substitution of α in place of a_1. It is now possible to replace the α and a_1 functions by the linear combinations of atomic orbitals given in equations (1) and (2) above. Since, however, only interactions with the central magnesium atom are being considered, at this stage it is only necessary to know the coefficients of the atomic orbitals which overlap with that atom, *i.e.* the oxygen orbitals numbered i in each Al_4O_4 cube, thus:

a_1 with respect to MgO_4, but derived from a_1 orbitals in Al_4O_4 cubes,

$$\psi_1 = 0.25(Ai + Bi + Ci + Di) \quad (4)$$

t_2 with respect to MgO_4, but derived from a_1 orbitals in Al_4O_4 cubes,

$$\psi_2 = 0.25(Ai + Bi - Ci - Di), \textit{ etc.} \quad (5)$$

a_1 with respect to MgO_4 but derived from α orbitals in Al_4O_4 cubes,

$$\psi_5 = 0.25\cdot(3)^{0.5}(Ai + Bi + Ci + Di) \quad (6)$$

t_2 with respect to MgO_4 but derived from α orbitals in Al_4O_4 cubes,

$$\psi_6 = 0.25\cdot(3)^{0.5}(Ai + Bi - Ci - Di), \textit{ etc.} \quad (7)$$

The a_1 orbitals will interact with the Mg 3*s* orbital whilst the t_2 orbitals will interact exclusively with the Mg 3*p* orbitals. In the limiting case of a wholly ionic bond between magnesium and oxygen, the (indefinitely small) Mg 3*p* coefficients associated with the ψ_2 and ψ_6 orbitals would be in the ratio $1 : 3^{0.5}$. This will be reduced by covalency so that the actual ratio of Mg 3*p* character in the two orbitals will be $1 : < 3$.

Correlations with X-Ray Emission and Photoelectron Spectra.—The model outlined above provides a rationalisation for the general form of the observed *X*-ray spectra and in particular for the striking difference in the shapes of the Mg-$K_{\beta_{1,3}}$ and Al-$K_{\beta_{1,3}}$ peaks. The two main features observed in all the three emission spectra are associated with the same m.o. energy levels. Since it is reasonable to assume that most electronic charge is associated with the oxygen atoms, the O-K_α emission spectrum will be discussed first. The distinct low-energy shoulder can be related to the a_1 orbitals in the Al_4O_4 units whilst the main peak would be derived from transitions from t_2 orbitals together with e, t_1, and t_2 orbitals tangential to Al_4O_4. Mutual repulsions between these orbitals will, however, cause a spread of ionisation energies, e being the most and t_1 the least tightly bound. If the differences in ionisation energies are only of the order of an electronvolt then the individual energy levels would not be observed as separate emission peaks with the resolution available in these experiments. Rather, as in the case of MgO, the peak associated with transitions from these orbitals will be distorted, with a low-energy tail.[9] This distortion is clearly visible in the O-K_α peak in the 522—523 eV region. This distortion has important implications when attempts are made to estimate the relative intensity of the low-energy feature at 521 eV. A simple resolution into Gaussian components is clearly not applicable: when due allowance is made for the distortion of the main peak the relative intensity of the peak at 521 eV is somewhat less than 10% of the principal peak, which is roughly what is anticipated by the Al_4O_4 model: for a_1, $(\sigma t_2 + e + t_1 + t_2) = 1 : 11$.

Aluminium 3*p* character is also associated with the a_1 and t_2 levels in Al_4O_4. The ionic limit of 3 : 1 is reduced, presumably by the presence of some degree of covalency in the Al–O band, to an observed value of *ca.* 1.2 : 1. It is interesting to note that the ratio is very similar to that observed in magnesium oxide (1 : 1),[9] suggesting that the shape of an *X*-ray emission peak may be used in a diagnostic way to determine co-ordination.

A very similar peak-intensity ratio is found (1.15 : 1) in the aluminium $L_{2,3}$ M spectrum which reflects the bonding role of the Al 3*s* orbital. In the simple m.o. model discussed above *sp* hybridisation was assumed which would require 3*s* character to behave in the same way as 3*p* character in all the molecular orbitals. Clearly, the experimental results support this model since the relative amounts of 3*s* and 3*p* character in the two main bands are the same and the energy of separation of the two component peaks is also the same (3.2 eV). The only point of difference is that the peaks in the *L* spectrum correspond to valence-band orbitals which are more tightly bound than those in the K_β spectrum by *ca.* 1 eV. Since the Al 3*s* orbital is more tightly bound than the Al 3*p* orbitals, this deviation from the oversimple ' hybrid-orbital ' approach is only to be expected.

The Mg-$K_{\beta_{1,3}}$ *X*-ray emission spectrum can be resolved into two main components which line up remarkably well with corresponding peaks in the oxygen and aluminium emission spectra and also the photoelectron spectra, confirming the validity of the model with two main bands of molecular orbitals. Whether the smaller peaks indicated by the curve resolution really reflect the existance of other less-intense orbital bands or merely deficiencies in both the experimental results and the resolution technique cannot be determined. It may be significant, however, that some evidence for other bands is to be found both in the oxygen emission spectrum and the photoelectron spectrum. Of rather greater significance is the very great difference in peak shape that is observed between the magnesium and aluminium emission peaks indicating that Mg 3*p* character is disposed between the two main bands in quite a different way from Al 3*p* character. This is, of course, what would be anticipated from the qualitative model discussed

above. The larger Mg $3p$ coefficient is associated with the m.o.s derived from the less tightly bound α orbitals, whilst a smaller coefficient is found in the more tightly bound orbitals. That the observed ratio is *ca.* 0.58 : 1, as compared with an ionic limit of 0.33 : 1 indicates some covalency in the Mg–O bands. The interaction of orbitals ψ_1 and ψ_4 with Mg $3s$ should be very similar to that found for Mg $3p$ orbitals so that the Mg-$L_{2,3}$ emission spectrum from spinel should be very similar to the $K_{\beta_{1,3}}$ spectrum (as is observed for MgO), but unfortunately it was not possible to measure the Mg-L spectrum from the sample of spinel used so that this prediction could not be investigated.

Whilst the valence-band photoelectron spectrum from the spinel sample from India shows only an oxygen $2s$ peak at 27 eV [Figure 1(*i*)], the synthetic crystal gave a distinct peak at 9.5 eV and a less-intense feature at 13.5 eV as well as a prominent oxygen $2s$ peak [Figure 1(*ii*)]. The peaks at 9.5 and 13.5 eV correlate well with the two main bands observed in the X-ray emission spectra. The photoelectric cross sections [19] for aluminium $3p$ electrons are only about one tenth of those for $3s$ electrons (Mg-K_α radiation) so that if similar cross-section behaviour is assumed for both Mg and Al $3s$ and $3p$ orbitals when irradiated with Al-K_α, the contributions to the photoelectron valence-band spectrum from the metal atoms in spinel will be dominated by $3s$ character. However, the cross section for oxygen $2p$ orbitals is only half that of Al $3s$ so that in a rather ionic bond, with a considerable proportion of the charge being located on the oxygen atoms, it is oxygen $2p$ character that will determine the photoelectron spectrum. This region of the photoelectron valence-band spectrum should, therefore, be very similar to the oxygen K_α X-ray emission spectrum and an examination of the spectra in Figure 1 shows this to be so. The most-intense peak in the valence-band photoelectron spectrum at *ca.* 27 eV correlates well with the $K_{\beta'}$ features in both the Al and Mg-$K_{\beta_{1,3}}$ spectra and also the low-energy satellite peak in the Al-L spectrum, confirming that these peaks reflect Al $3p$, Mg $3p$, and Al $3s$ character in m.o.s that are predominantly oxygen $2s$.

Conclusions.—The combination of X-ray emission and X-ray photoelectron spectra from spinel enables the electronic structure of the molecular orbitals to be determined. Three main bands are observed with binding energies of *ca.* 10, 13.5, and 27 eV (relative to a carbon $1s$ energy of 288 eV). The least tightly bound orbitals are mostly oxygen $2p$ in character, whilst the band at 27 eV is almost exclusively oxygen $2s$. Calculations based on simple m.o. theory enable the disposition of Al and Mg $3s$ and $3p$ valence-shell orbitals amongst the various m.o.s of spinel to be rationalised. Aluminium $3s$ and $3p$ character are both found in both of the least tightly bound orbitals, but somewhat more is present in the band of 13.5 eV than in that at 10 eV. This is reversed for Mg $3p$ orbitals and reflects the different bonding situation of the aluminium and magnesium atoms in the spinel lattice. The difference in emission peak profiles is such that it should be possible to distinguish between atoms at the four- and six-coordinate sites in spinel.

We thank the Royal Society, the S.R.C., and the Central Research Fund of London University for assistance in the purchase of spectrometers, and the Scientific Affairs Division of N.A.T.O. for the award of a research grant to study soft X-ray spectra. We also gratefully acknowledge the help of Dr. Scopes, Westfield College, University of London for the use of the Du Pont 310 curve resolver, and of Dr. Bishop, British Museum (Natural History) and of Professor J. C. Anderson, Imperial College (Electrical Engineering) for samples of spinel. C. J. N., M. J. W., and D. E. H. all thank the S.R.C. for the awards of postgraduate research grants.

[7/2156 *Received*, 8*th December*, 1977]

[19] J. H. Scofield, Lawrence Livermore Laboratory, Report UCRL-51326.